

# [<sup>3</sup>H](Azidophenyl)ureido Taxoid Photolabels Peptide Amino Acids 281–304 of $\alpha$ -Tubulin<sup>†</sup>

C. Loeb,<sup>‡</sup> C. Combeau,<sup>§</sup> L. Ehret-Sabatier,<sup>‡</sup> A. Breton-Gilet,<sup>§</sup> D. Faucher,<sup>§</sup> B. Rousseau,<sup>||</sup> A. Commerçon,<sup>§</sup> and M. Goeldner<sup>\*,‡</sup>

Laboratoire de Chimie Bio-organique, URA 1386 CNRS, Faculté de Pharmacie, Université Louis Pasteur Strasbourg, BP 24, 67401 Illkirch cedex, France, Rhône-Poulenc Rorer SA, Centre de Recherches de Vitry-Alfortville, 13 Quai Jules Guesde, 94403 Vitry sur Seine, France, and Service des Molécules Marquées Département de Biologie Cellulaire et Moléculaire, CEA Saclay, 91191 Gif sur Yvette, France

Received July 2, 1996; Revised Manuscript Received December 2, 1996<sup>⊗</sup>

**ABSTRACT:** The taxoid binding site on porcine brain tubulin was covalently labeled, in the presence or absence of Taxotere, with the photoaffinity reagent [<sup>3</sup>H]-*p*-(azidophenyl)ureido taxoid derivative [<sup>3</sup>H]-TaxAPU [Combeau, C., Commerçon, A., Mioskowski, C., Rousseau, B., Aubert, F., & Goeldner, M. (1994) *Biochemistry* 33, 6676–6683]. After disulfide reduction and carboxymethylation, the alkylated tubulin samples were treated with trypsin and the mixtures of peptides were first fractionated by gel filtration over Sephadex G50. Anion exchange chromatography of the radioactive areas showed, for one area, three major radioactive signals which were further analyzed by reversed phase C18 HPLC, leading to well-resolved radioactive peaks. Microsequencing of these different peaks gave a complete sequence of a tryptic fragment on  $\alpha$ -tubulin ( $\alpha$ -281–304) and two partial peptide sequences of a tryptic fragment on  $\beta$ -tubulin ( $\beta$ -217–229) in addition to sequences of mixture of peptides. The radioactive signals were lost while concentrating the samples for microsequencing, preventing the identification of the modified amino acids. These results identify the first peptide on  $\alpha$ -tubulin which binds to the taxoids and confirm the involvement of both  $\alpha$ - and  $\beta$ -tubulin in the taxoid binding site.

Microtubules, the most prominent elements in the spindle apparatus, are the target of many antimitotic drugs. Among the numerous tubulin-interacting drugs, Taxol<sup>1</sup> and its semisynthetic analogue Taxotere (Guérin-Voegelein *et al.*, 1991) exhibit the unique property of promoting tubulin assembly and preventing microtubules from cold-induced depolymerization (Schiff *et al.*, 1979; Parness & Horwitz, 1981; Ringel & Horwitz, 1991). The stabilization of microtubules by taxoids is thought to be the basis for their cytotoxicity (Jordan *et al.*, 1993). Taxol and Taxotere have undergone very promising clinical trials and have been approved by the U.S. Food and Drug Administration for the treatment of advanced ovarian and advanced breast cancers, respectively. Thus, taxoids constitute an important new class of antitumor agents (Guénard *et al.*, 1995).

The existence of only one taxoid binding site per  $\alpha/\beta$ -subunit dimer on the polymer (Parness & Horwitz, 1981; Diaz & Andreu, 1993) has promoted a series of structural investigations to define the taxoid binding site on tubulin. To address this question, several taxoid-derived photoaffinity probes have been designed and synthesized (Georg *et al.*, 1992, 1994, 1995a; Carboni *et al.*, 1993; Rimoldi *et al.*, 1993; Swindell *et al.*, 1994). Furthermore, different radiolabeled probes have led to the identification of the tubulin subunits and peptide fragments involved in the recognition of taxoids. Successively, [<sup>3</sup>H]Taxol was used directly and was shown to photolabel the  $\beta$ -subunit (Rao *et al.*, 1992) and then a 3'-*p*-(azidobenzamido) Taxol labeled the N-terminal 31 amino acids of  $\beta$ -tubulin (Rao *et al.*, 1994), while independently, the same probe was shown to label both  $\alpha$ - and  $\beta$ -subunits with a predominance for  $\beta$ -tubulin using MAP-free tubulin (Dasgupta *et al.*, 1994). Another taxoid probe, modified on the side chain 3'-position, *p*-(azidophenyl)ureido derivative (TaxAPU), had already been shown to label predominantly  $\beta$ - over  $\alpha$ -tubulin (Combeau *et al.*, 1994). More recently, a 2-substituted *m*-azidobenzoyl Taxol probe was shown to label peptide amino acids 217–231 on  $\beta$ -tubulin (Rao *et al.*, 1995). Clearly, these labeling results, somehow controversial, will have to be analyzed with respect to the newly described three-dimensional reconstruction of zinc-induced assembled tubulin (6.5 Å resolution) which proposed a positioning of the Taxol binding site on the  $\beta$ -subunit (Nogales *et al.*, 1995).

In the present study, we show that the labeling of purified tubulin with [<sup>3</sup>H]TaxAPU (Figure 1) occurs on the tryptic fragment of amino acids 281–304 of  $\alpha$ -tubulin, while a partial identification of the peptide of amino acids 217–

<sup>†</sup> This work was supported by the Centre National de la Recherche Scientifique, the Association pour la Recherche sur le Cancer, and the Fondation de France.

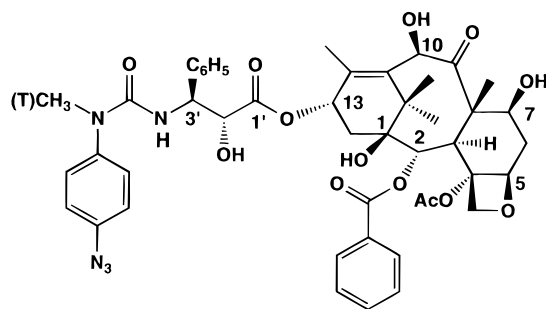
<sup>‡</sup> Université Louis Pasteur Strasbourg.

<sup>§</sup> Rhône-Poulenc Rorer SA.

<sup>||</sup> CEA Saclay.

<sup>⊗</sup> Abstract published in *Advance ACS Abstracts*, March 15, 1997.

<sup>1</sup> Abbreviations: TaxAPU, [(azidophenyl)ureido]taxane derivative; Taxol (paclitaxel), 4,10-diacetoxy-2 $\alpha$ -(benzoyloxy)-5 $\beta$ ,20-epoxy-1,7 $\beta$ -dihydroxy-9-oxotax-11-en-13 $\alpha$ -yl (2R,3S)-3-[(phenylcarbonyl)amino]-2-hydroxy-3-phenylpropionate; Taxotere (docetaxel, trademark of Rhône-Poulenc Rorer RP56976), 4-acetoxy-2 $\alpha$ -(benzoyloxy)-5 $\beta$ ,20-epoxy-1,7 $\beta$ ,10 $\beta$ -trihydroxy-9-oxotax-11-en-13 $\alpha$ -yl (2R,3S)-3-[(*tert*-butoxycarbonyl)amino]-2-hydroxy-3-phenylpropionate; Tris, tris(hydroxymethyl)aminomethane; MES, 2-(*N*-morpholino)ethanesulfonic acid; GTP, guanosine 5'-triphosphate; TFA, trifluoroacetic acid; EGTA, [ethylenebis(oxyethylenenitrilo)]tetraacetic acid; SDS, sodium dodecyl sulfate; DTT, dithiothreitol; MAP, microtubule-associated protein; HPLC, high-performance liquid chromatography.

FIGURE 1: [ $^3\text{H}$ ]TaxAPU.

229 of  $\beta$ -tubulin was also observed. These results, in agreement with previous labeling results obtained on  $\beta$ -tubulin (Rao *et al.*, 1995), ensure the contribution of  $\alpha$ -tubulin in the taxoid binding site (Combeau *et al.*, 1994; Dasgupta *et al.*, 1994).

## MATERIALS AND METHODS

### Chemicals.

Tris was from Euromedex. MES came from Calbiochem. GTP and trypsin were purchased from Boehringer Mannheim. Electrophoresis materials and reagents were from BioRad. HPLC grade  $\text{CH}_3\text{CN}$  was from Merck. TFA came from Fluka. All other reagents were from Sigma. [ $^3\text{H}$ ]TaxAPU was synthesized as initially described (Combeau *et al.*, 1994) (specific activity of 1 Ci/mmol). Taxotere (docetaxel, RP 56976) was from Rhône-Poulenc Rorer.

### Preparation of Microtubule Protein and Pure Tubulin

Microtubule protein was isolated from porcine brain by two cycles of polymerization–depolymerization (Shelanski *et al.*, 1973). Pure tubulin was separated from MAPs after a phosphocellulose P11 chromatography of microtubule protein cycled three times (Weingarten *et al.*, 1975). The protein solutions were stored at  $-80^\circ\text{C}$  in a buffer consisting of 50 mM MES/NaOH (pH 6.8), 0.25 mM  $\text{MgCl}_2$ , 0.5 mM EGTA (RB/2 buffer) with 3.4 M glycerol, and 0.2 mM GTP.

### Photoaffinity Labeling

For irradiation experiments, microtubule protein (3–4 mg/mL) was cycled as follows. Polymerization was achieved in 30 min at  $37^\circ\text{C}$  in the presence of 1 mM GTP. Microtubules were sedimented at  $220000g$  for 50 min and at  $37^\circ\text{C}$ . The pellet was resuspended in RB buffer [100 mM MES/NaOH (pH 6.8), 0.5 mM  $\text{MgCl}_2$ , and 1 mM EGTA] at  $4^\circ\text{C}$ , and the solution was clarified by a centrifugation at  $220000g$  for 25 min. Cycled microtubule protein (1.4 mL, 12  $\mu\text{M}$ ) was polymerized for 30 min in the dark at  $37^\circ\text{C}$  in RB buffer supplemented with 1 mM  $\text{MgCl}_2$ , 30  $\mu\text{M}$  GTP, and 10  $\mu\text{M}$  [ $^3\text{H}$ ]TaxAPU. The solution was irradiated at 266 nm for 10 min using a monochromatic light beam (light energy of  $87 \times 10^{-9}$  einstein  $\text{s}^{-1} \text{cm}^{-2}$ ). For comparison, the same experiment was performed with pure microtubules as previously described (Combeau *et al.*, 1994).

### SDS–PAGE Analysis

After denaturation, the irradiated microtubules (20  $\mu\text{g}$ ) were loaded on a 5–15% acrylamide gel and processed for a 20 h electrophoresis at 50 V. The gel was stained with Coomassie blue R. Each gel lane was cut in 2.2 mm slices

which was digested with 250  $\mu\text{L}$  of 30% hydrogen peroxide during 16 h at  $85^\circ\text{C}$ . After the solution was cooled at room temperature, 300  $\mu\text{L}$  of 4 M urea in 1% SDS and 4.5 mL of scintillation cocktail (emulsifier-safe from Packard) were added to the digested slices. The samples were counted after a vigorous shaking.

### Preparative Photoaffinity Labeling of Pure Microtubules for Peptide Isolation

A total of 18 mg of pure microtubules was irradiated. Each time, 1.4 mL of pure microtubules (12  $\mu\text{M}$ ) and [ $^3\text{H}$ ]TaxAPU (6.7  $\mu\text{M}$ ) were irradiated in the presence or absence of Taxotere (0.1 mM). After irradiation, the microtubules were sedimented for 50 min at  $220000g$  and  $37^\circ\text{C}$ . The pellet was resuspended in a dissociated buffer consisting of 0.5 M Tris-HCl (pH 8.5) containing 8 M urea. The dissociated tubulin was reduced with 2 mM DTT for 3 h at room temperature under argon. Tubulin was then carboxymethylated with 1.5 equiv of iodoacetic acid dissolved in 0.5 M NaOH. The reaction proceeded for 1 h in darkness. Finally, tubulin free of unbound [ $^3\text{H}$ ]TaxAPU and excess reagents was obtained by chromatography of the mixture over a Sephadex G25 column (Pharmacia) ( $1.2 \times 30$  cm). The elution was performed with 50 mM  $\text{NH}_4\text{HCO}_3$  at a flow rate of 0.2 mL/min. Fractions of 1 mL were collected, each of which were checked for absorption at 280 nm and for tritium radioactivity. The tubulin fractions were pooled and concentrated with a Centricon-30 device (Amicon). The final protein concentration was measured with a Bradford assay (BioRad protein assay).

Similar labeling experiments were achieved on preformed microtubules assembled from a 12  $\mu\text{M}$  solution during 15 min at  $37^\circ\text{C}$  in the presence of 6 mM  $\text{MgCl}_2$  and 20  $\mu\text{M}$  GTP. After that, [ $^3\text{H}$ ]TaxAPU (6.7  $\mu\text{M}$ ) was added before irradiation in the presence or absence of Taxotere (0.1 mM).

### Radiolabeled Peptide Purification

**Proteolysis.** Tubulin (3 mg/mL) in 50 mM  $\text{NH}_4\text{HCO}_3$  was digested for 24 h at  $37^\circ\text{C}$  upon two successive additions of trypsin [a total of 4% (w/w) was added].

**Gel Filtration Chromatography.** Tryptic digests were loaded onto a Sephadex G50 column (Pharmacia) ( $1.6 \times 62$  cm). Peptides were eluted at a flow rate of 0.2 mL/min with 100 mM  $\text{NH}_4\text{HCO}_3$  containing 8 M urea. Fractions (2 mL) were collected, and an aliquot of each fraction was assayed for radioactivity.

**Anion Exchange Chromatography.** The fractions of each radioactive area were pooled and desalted using Sep-Pak C18 cartridges. Peptides were eluted with 60%  $\text{CH}_3\text{CN}$  in water. After evaporation of  $\text{CH}_3\text{CN}$  under vacuum with a Speedvac device, the samples were loaded onto a MonoQ HR 5/5 column (Pharmacia). Peptides were eluted at a flow rate of 1 mL/min with solvent A (10%  $\text{CH}_3\text{CN}$  in 10 mM Tris-HCl at pH 8.0) and solvent B (solvent A with 1 M NaCl) as follows: solvent A at 100% for 0–5 min and then a linear increase of solvent B from 0% at 5 min to 50% at 65 min. Fractions were collected every 0.5 min and assayed for radioactivity. Absorbance was monitored on-line at 214 nm.

**Reversed Phase Chromatography.** The fractions of each radioactive peak were pooled. TFA was added to a final concentration of 0.1%, and the samples were loaded on a C18 HPLC column ( $250 \times 4.6$  mm, Vydac). Elution was

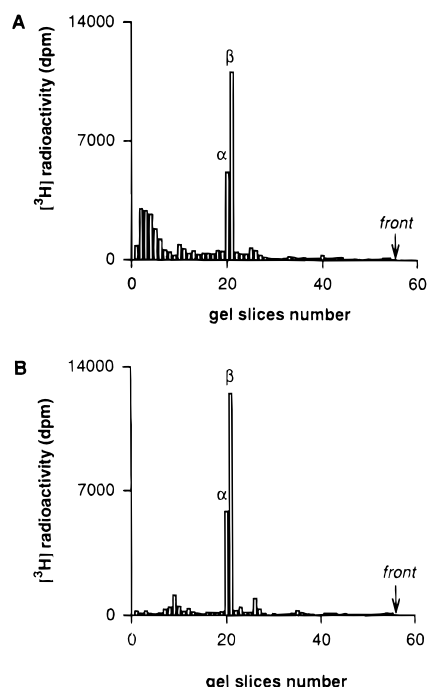


FIGURE 2: Specific radioactivity incorporation of [ $^3\text{H}$ ]TaxAPU into microtubules upon irradiation. Microtubules were irradiated with [ $^3\text{H}$ ]TaxAPU (10  $\mu\text{M}$ ) with or without Taxotere (0.3 mM). Samples were denatured and subjected to electrophoresis on a 5–15% SDS–acrylamide gel (total tubulin loaded, 20  $\mu\text{g}$ ). The gel lane was cut into slices which were digested and counted. The difference of radioactivity in the absence and presence of Taxotere is the specific radioactivity incorporation. The specific incorporation is reported for (A) microtubule protein and (B) MAPs-free microtubules. Arrows indicate the front of gels.

performed at a flow rate of 1 mL/min with solvent C (0.1% TFA in water) and solvent D (0.1% TFA in  $\text{CH}_3\text{CN}$ ). For peak  $b_1$ , the elution started with 80% solvent C followed by a linear gradient to 45% solvent D in 100 min. For peaks  $b_2$  and  $b_3$ , the elution started with 98% solvent C during 10 min, followed by a linear gradient to 20% solvent D in 20 min, an isocratic elution during 20 min, a linear gradient to 30% solvent D in 30 min, an isocratic elution during 20 min, a linear gradient to 40% solvent D in 30 min, and finally an isocratic elution during 10 min. The absorbance was monitored on-line at 214 nm. Fractions were collected every minute, and an aliquot was assayed for radioactivity. Sequencing analysis was carried out on an Applied Biosystems 494 sequencer.

## RESULTS

**Photolabeling of Tubulin Using [ $^3\text{H}$ ]TaxAPU in the Presence of MAPs.** Microtubule protein-containing microtubules plus associated proteins (MAPs) were photolabeled in the presence of 10  $\mu\text{M}$  [ $^3\text{H}$ ]TaxAPU as indicated in Materials and Methods. The photolabeling experiment was compared with a MAP-free tubulin photolabeling experiment after gel electrophoresis and quantification of the radioactivity incorporated along the gel (Figure 2).

**Photolabeling of Tubulin Using [ $^3\text{H}$ ]TaxAPU for Peptide Identification.** Purified tubulin was photolabeled by [ $^3\text{H}$ ]TaxAPU in the presence or absence of 0.1 mM Taxotere as indicated in Materials and Methods. The 6.7  $\mu\text{M}$  concentration of the probe was selected according to Combeau *et al.* (1994) to permit high incorporation of radioactivity with a

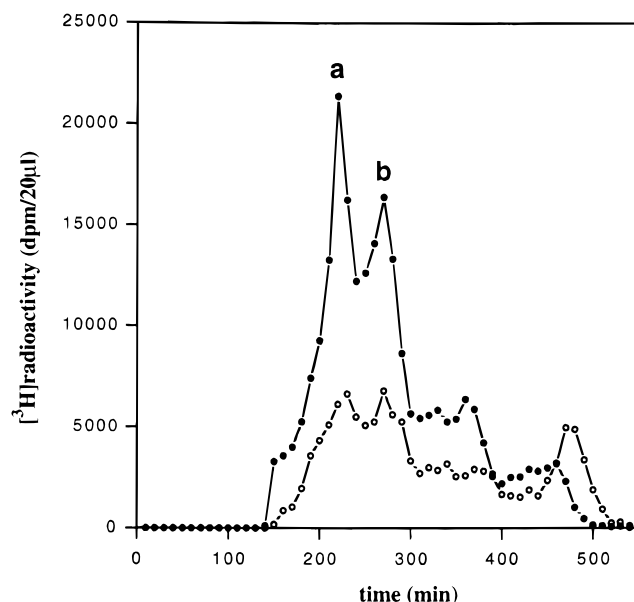


FIGURE 3: Gel filtration chromatography of tryptic tubulin peptides. Tryptic digests of [ $^3\text{H}$ ]TaxAPU-photolabeled tubulin (6.8 mg) [in the presence (○) or absence (●) of 0.1 mM Taxotere] were applied to a Sephadex G50 column. Elution conditions are described in Materials and Methods.

good signal/noise ratio. The quantity of photolabeled tubulin (18 mg) was chosen to have sufficient material for the overall purification and sequencing steps.

After removal of excess tritiated probe, the carboxymethylated tubulin was further purified by gel filtration on Sephadex G25. A clear separation between tubulin (not modified or radiolabeled) from other constituents such as GTP and the photodecomposed probe was observed (not shown).

**Photolabeling Experiments with [ $^3\text{H}$ ]TaxAPU on Pre-formed Microtubules.** Preformed microtubules were photolabeled with [ $^3\text{H}$ ]TaxAPU in the presence or absence of 0.1 mM Taxotere. This experiment was analyzed by gel electrophoresis and quantification of the radioactivity incorporated along the gel showing an 81% specific incorporation in the  $\alpha$ -subunit and 76% in the  $\beta$ -subunit with a  $\beta/\alpha$  ratio of 1.6.

**Trypsin Digestion and Peptide Purification.** Radiolabeled tubulin samples were subjected to two successive trypsinolysis experiments. The mixtures of peptides were first fractionated by gel filtration on Sephadex G50 (Figure 3), giving reproducible elution patterns for radioactive areas a and b. The lower-molecular weight area showed variability in its relative content of radioactivity along the different experiments and was not further investigated. Anion exchange chromatography of radioactive materials in areas a (not shown) and b (Figure 4) showed, only in the latter case, well-resolved radioactive peaks. Area a gave a more complicated pattern which will require additional proteolysis and purification steps for satisfactory analysis. Similar results were obtained from the analysis of photolabeled preformed microtubules showing identical G50 and anion exchange profiles with higher protection patterns (not shown).

The peaks resulting from the anion exchange chromatography of area b (Figure 4) were further analyzed by reversed phase C18 HPLC. The most interesting radioactivity profiles (Figure 5A–C) were observed within fractions  $b_1$ ,  $b_2$ , and

Table 1: Amino Acid Sequences from the Different Purified Peptides

peak number	fraction number	sequence
peak b <sub>1</sub>	fraction 73	$\beta$ -217–229, (–)(–)(–)PT Y G D L N(–)LV
	fraction 77	no peptide sequence
peak b <sub>2</sub>	fraction 80	no peptide sequence
	fraction 114	$\beta$ -217–229, (–) T (–) P T Y G (–) L (–) (–) LV
peak b <sub>3</sub>	fraction 70	$\alpha$ -281–304, A Y H E Q L S V A E I T N A (–) F E P A N Q M V K
	fraction 84	$\alpha$ -167–185, L E F S I Y P A P Q V S T A V V E P Y
		$\beta$ -283–302, A L T V P E L T Q Q M F D A (–) N M M A A

<sup>a</sup> (–), residue not found.

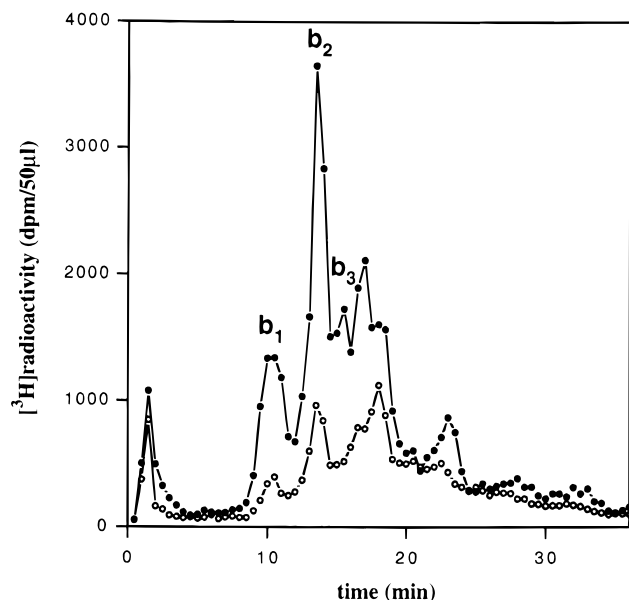


FIGURE 4: Anion exchange chromatography of peak b [in the presence (O) or absence (●) of 0.1 mM Taxotere]. Pooled radioactive fractions of peak b from gel filtration (0.86 mg) were desalted and then applied to an anion exchange column. Elution was developed as described in Materials and Methods.

b<sub>3</sub>, each showing well-resolved radioactive peaks: fractions 73 and 77 from b<sub>1</sub> (Figure 5A), fractions 80 and 114 from b<sub>2</sub> (Figure 5B), and fractions 70 and 84 from b<sub>3</sub> (Figure 5C). Successive HPLC injections were necessary to collect sufficient material for microsequencing experiments.

**Microsequencing of Purified Peptides.** Table 1 summarizes the sequencing results. No peptide sequence was detected within fractions 77 from peak b<sub>1</sub> and 80 from peak b<sub>2</sub>, while partial sequences over 13 cycles corresponding to amino acids 217–229 of  $\beta$ -tubulin were detected in fractions 73 (b<sub>1</sub>) and 114 (b<sub>2</sub>). Further sequencing of these peptides did not furnish additional amino acid identification. The C18 HPLC fraction 70 from peak b<sub>3</sub> showed a full sequence of a single peptide corresponding to complete tryptic fragment  $\alpha$ -281–304. As expected, within this sequence, Cys 295 was not identified after chemical modification (see Materials and Methods). Finally, fraction 84 within b<sub>3</sub> contained a mixture of two peptide sequences, corresponding to partial tryptic fragments  $\beta$ -283–302 and  $\alpha$ -167–185.

## DISCUSSION

In the presence of taxoids, tubulin polymerizes without GTP, leading to stable microtubules. In contrast to other antimitotic alkaloids, Taxol and Taxotere associate specifically and reversibly to microtubules ( $K_d \sim 1 \mu\text{M}$ ) with a stoichiometry of 1 per  $\alpha/\beta$ -assembled tubulin (Parness & Horwitz, 1981; Diaz & Andreu, 1993). The binding site of

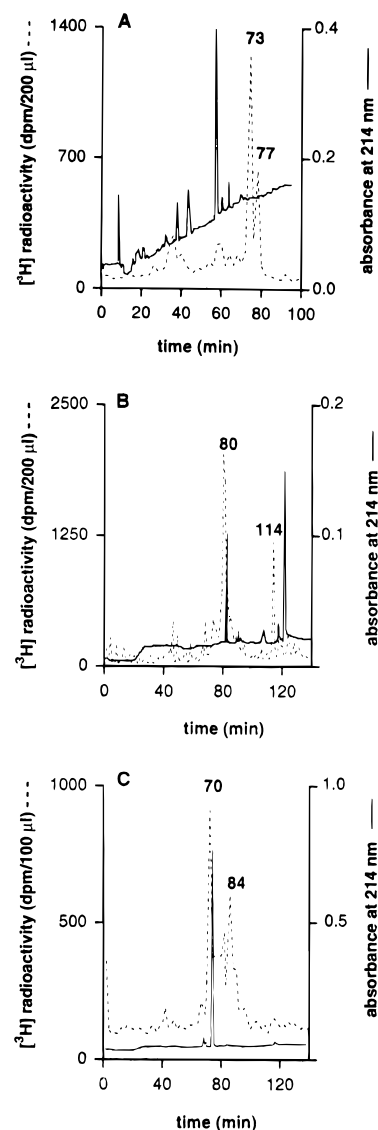


FIGURE 5: Reversed phase HPLC separation of peptides from peaks b<sub>1</sub> (A), b<sub>2</sub> (B), and b<sub>3</sub> (C). Pooled radioactive fractions from anion exchange chromatography were loaded directly onto a C18 reversed phase column. See Materials and Methods.

taxoids on microtubules remains to be defined, and photoaffinity labeling was chosen in the first instance to investigate this interaction. Photoaffinity labeling methodology can lead to a molecular characterization of a ligand binding site by the identification of the peptides and ultimately the amino acids constituting the site (Kotzyba-Hibert *et al.*, 1995). Several photoaffinity probes with photoreactive groups at different positions on the Taxol skeleton have been designed and synthesized (Georg *et al.*, 1995b). At first, a direct photo-cross-linking of radiolabeled Taxol to tubulin was described to occur on the  $\beta$ -subunit of tubulin (Rao *et al.*,

1992). The photocoupling approach using a natural ligand, without modification with photoreactive groups, has been used in many instances (Bouchet & Goeldner, 1997) but gives generally very low coupling yields, and this was the case for Taxol. A series of C-7-modified probes also gave unsatisfactory photolabeling results (Rimoldi *et al.*, 1993); in particular, the specificity of radioactive incorporation could not be demonstrated for these probes. The incorporation of arylazido groups in the C-13 Taxol side chain on position C-3' gave the first reliable photoaffinity labeling results. [<sup>3</sup>H]-3'-(*p*-Azidobenzamido) Taxol was described to label exclusively  $\beta$ -tubulin with the N-terminal 31 amino acids as the major site for photo-cross-linking (Rao *et al.*, 1994). However, the same probe was shown to label predominantly  $\beta$ - over  $\alpha$ - tubulin subunits (Dasgupta *et al.*, 1994) on pure microtubules. Another taxoid probe modified on the side chain 3'-position, the [<sup>3</sup>H]-*p*-(azidophenyl)ureido derivative ([<sup>3</sup>H]TaxAPU), had already been shown to label predominantly  $\beta$ - over  $\alpha$ -tubulin, again on pure microtubules (Combeau *et al.*, 1994). Finally, a 2-substituted [<sup>3</sup>H]-*m*-azidobenzoyl Taxol probe was shown to label peptide amino acids 217–231 on  $\beta$ -tubulin (Rao *et al.*, 1995).

Taken together, the different photoaffinity labeling results do not permit one to assign the taxoid binding site to a given tubulin subunit. While the  $\beta$ -subunit seems to play a dominant role in the taxoid recognition, the  $\alpha$ -subunit cannot be excluded. To determine the possible influence of MAPs on this interaction, we photolyzed tubulin successively in the presence and in the absence of MAPs with [<sup>3</sup>H]TaxAPU, in comparable conditions, using a quantitative method of radioactivity detection on the gel electrophoresis rather than autoradiography. Although specific incorporation of radioactivity corresponding to higher-molecular weight species is observed in the former case (Figure 2A), and for which we do not have a satisfactory explanation, i.e. cross-linking of labeled tubulin with MAPs might occur at the used wavelength, the labeling results did not show major differences either for the total amount of radioactivity incorporated in both subunits or for the  $\alpha/\beta$  labeling ratio (Figure 2A,B). We also checked the influence of the polymerized state of tubulin by analyzing the labeling of preformed microtubules with [<sup>3</sup>H]TaxAPU (not shown). Clearly, an increase in specific radioactivity incorporation (81% in the  $\alpha$ -subunit and 76% in the  $\beta$ -subunit) was observed when compared to the labeling of [<sup>3</sup>H]TaxAPU-induced polymers (Combeau *et al.*, 1994). Also, a decrease in the  $\beta/\alpha$  ratio is observed, going from 2.5 to 1.6. This experiment emphasizes the contribution of the  $\alpha$ -subunit in the taxoid binding site.

To precisely define the molecular interaction between the [<sup>3</sup>H]TaxAPU probe and tubulin, we analyzed the location of the taxoid on the tubulin sequence by proteolysis of the protein and identification of the radiolabeled peptides. Preliminary experiments using thrombin as a proteolytic enzyme indicated a loss of peptide-associated radioactivity while concentrating the solutions. We were not able to prevent satisfactorily this loss, whatever the conditions used (pH, temperature). Clearly, this azido probe did not form a stable bond with the protein. This can occur when chemical bonds are formed between nucleophilic protein residues and the rearranged azido probe, i.e. didehydroazepine species resulting from singlet nitrenes, and which regenerate the initial peptide in hydrolytic conditions (Bayley, 1983; Kotzyba-Hibert *et al.*, 1995). To overcome this problem of

radioactivity loss, we decided first to use trypsin as a proteolytic agent to obtain directly small peptide fragments, second to cleave tubulin as a mixture of subunits to have sufficient material at disposal for the complete purification procedures, and finally to avoid, as much as possible, concentration of the reaction mixture to dryness.

The purification procedure could be noticeably improved by performing, prior to C18 reversed phase HPLC, anion exchange chromatography which showed for one radioactive area (area b, Figure 3) well-resolved radioactive peaks on the chromatogram (Figure 4). Peaks b<sub>1</sub>–b<sub>3</sub>, which possessed higher specific radioactivity incorporation (Figure 4), were further purified by reversed phase HPLC, leading in each case to well-resolved single radioactive fractions (Figure 5A–C). During microsequencing of these different fractions (Table 1), none released radioactivity during the cycles, confirming that the loss of radioactivity occurred through concentration to dryness of the radioactive HPLC fractions before microsequencing (not shown). Fraction 70 from peak b<sub>3</sub> (Figure 5C) led to the full peptide sequence of complete tryptic fragment  $\alpha$ -281–304. This is the first peptide identified on  $\alpha$ -tubulin to contribute to the taxoid binding site. Analyses of fractions 73 from peak b<sub>1</sub> (Figure 5A) and 114 from peak b<sub>2</sub> (Figure 5B) each gave a partial peptide sequence of a tryptic fragment on  $\beta$ -tubulin ( $\beta$ -217–229). Interestingly, these partial sequences overlap with a cyanogen bromide/tryptic fragment  $\beta$ -217–231 described as the major photolabeled peptide from [<sup>3</sup>H]-2-(*m*-azidobenzoyl) Taxol (Rao *et al.*, 1995). Fraction 84 from peak b<sub>3</sub> (Figure 5C) gave a mixture of two peptides from  $\alpha$ - and  $\beta$ -tubulin, and it is not possible to attribute the initial radioactive signal to either peptide. Finally, the analyses of the two remaining fractions, 77 from peak b<sub>1</sub> (Figure 5A) and 80 from peak b<sub>2</sub> (Figure 5B), gave no peptide sequence, and we have no satisfactory explanation for this fact.

The specificity of labeling was shown throughout the different purification procedures, leading to the ultimate  $\alpha$ -281–304 peptide identification. The experimental conditions used (12  $\mu$ M tubulin for 6.7  $\mu$ M probe, assuming a  $K_d$  of 6  $\mu$ M) indicate that almost half of the probe is reversibly bound to the protein, which should therefore limit the nonspecific labeling. Clearly, during the protection experiment (labeling in the presence of 0.1 mM Taxotere), the radioactivity incorporation could not be fully prevented. Along the different purification steps, increasing amounts of protection were observed: 40% after G25 filtration (not shown), 63% (peak a) and 54% (peak b) after G50 chromatography (Figure 3), and up to 75% in peaks b<sub>1</sub>–b<sub>3</sub> after ion chromatography (Figure 4). The specificity of labeling was directly dependent on the Taxotere concentration (Combeau *et al.*, 1994), but we could not use higher Taxotere concentrations mainly because of its solubility limit.

Our labeling results confirm at first the contribution of both  $\alpha$ - and  $\beta$ -tubulin in the taxoid binding site on microtubules. Clearly, the proposed location of the Taxol binding site on the zinc-induced assembled tubulin (Nogales *et al.*, 1995) partially contradicts this result. However, the contacts between subunits and the subsequent localization of the Taxol binding site might differ in intact microtubules and zinc sheets (Makowski, 1995). Our results also suggest that the 3'-substituted TaxAPU derivative may adopt a conformation which differs from the other 3'-substituted photoaffinity probe [[<sup>3</sup>H]-3'-(*p*-azidobenzamido) Taxol which photolabeled

the N-terminal part of the  $\beta$ -subunit (Rao *et al.*, 1994)]. To address this question, we currently model the three-dimensional structure of these taxoid photoaffinity probes to study the influence of the 3'-side chain chemical modifications on their overall conformation. Photoaffinity labeling studies will bring new insight in the conformational analyses of Taxol derivatives within their tubulin binding site.

## ACKNOWLEDGMENT

We thank Dr. François Lavelle for constant interest in this work.

## REFERENCES

- Bayley, H. (1983) in *Laboratory Techniques in Biochemistry and Molecular Biology* (Work, T. S., & Burton, R. H., Eds.) Vol. 12, p 34, Elsevier, Amsterdam.
- Bouchet, M.-J., & Goeldner, M. (1997) *Photochem. Photobiol.* (in press).
- Carboni, J. M., Farrina, V., Rao, S., Hauck, S. I., Horwitz, S. B., & Ringel, I. (1993) *J. Med. Chem.* 36, 513–515.
- Combeau, C., Commerçon, A., Mioskowski, C., Rousseau, B., Aubert, F., & Goeldner, M. (1994) *Biochemistry* 33, 6676–6683.
- Dasgupta, D., Park, H., Harriman, G. C. B., Georg, G. I., & Himes, R. H. (1994) *J. Med. Chem.* 37, 2976–2980.
- Diaz, J. F., & Andreu, J. M. (1993) *Biochemistry* 32, 2747–2755.
- Georg, G. I., Harriman, G. C. B., Himes, R. H., & Mejillano, M. R. (1992) *Bioorg. Med. Chem. Lett.* 2, 735–738.
- Georg, G. I., Harriman, G. C. B., Park, H., & Himes, R. H. (1994) *Bioorg. Med. Chem. Lett.* 4, 487–490.
- Georg, G. I., Boge, T. C., & Park, H. (1995a) *Bioorg. Med. Chem. Lett.* 5, 615–620.
- Georg, G. I., Boge, T. C., Cheruvallath, Z. S., Clowers, J. S., Harriman, G. C. B., Hepperle, M., & Park, H. (1995b) in *Taxol Science and applications* (Suffness, M., Ed.) pp 317–375, CRC Press, Boca Raton, FL.
- Guénard, D., Guéritte-Voegelein, F., & Lavelle, F. (1995) *Curr. Pharm. Des.* 1, 95–112.
- Guéritte-Voegelein, F., Guénard, D., Lavelle, F., Legoff, M., Mangatal, L., & Potier, P. (1991) *J. Med. Chem.* 34, 992–998.
- Jordan, M. A., Toso, R. J., Thrower, D., & Wilson, L. (1993) *Proc. Natl. Acad. Sci. U.S.A.* 90, 9552–9556.
- Kotzyba-Hibert, F., Kapfer, I., & Goeldner, M. (1995) *Angew. Chem., Int. Ed. Engl.* 34, 1296–1312.
- Lavelle, F. (1993) *Curr. Opin. Invest. Drugs* 2, 627–635.
- Makowski, L. (1995) *Nature* 375, 361–362.
- Nogales, E., Wolf, S. G., Khan, I. A., Luduena, R. F., & Downing, K. H. (1995) *Nature* 375, 424–427.
- Parness, J., & Horwitz, S. B. (1981) *J. Cell Biol.* 91, 479–487.
- Rao, S., Horwitz, S. B., & Ringel, I. (1992) *J. Natl. Cancer Inst.* 84, 785–788.
- Rao, S., Krauss, N. E., Heerding, J. M., Swindell, C. S., Ringel, I., Orr, G. A., & Horwitz, S. B. (1994) *J. Biol. Chem.* 269, 3132–3134.
- Rao, S., Orr, G. A., Chaudhary, A. G., Kingston, D. G. I., & Horwitz, S. B. (1995) *J. Biol. Chem.* 270, 20235–20238.
- Rimoldi, J. M., Kingston, D. G. I., Chaudhary, A. G., Saramaniak, G., Grover, S., & Hamel, E. (1993) *J. Nat. Prod.* 56, 1313–1330.
- Swindell, C. S., Heerding, J. M., Krauss, N. E., Horwitz, S. B., Rao, S., & Ringel, I. (1994) *J. Med. Chem.* 37, 1446–1449.

BI961602R